Laser and Particle Beams (2016), *34*, 1–10.

doi:10.1017/S0263034615000749

Second-harmonic generation by relativistic self-focusing of cosh-Gaussian laser beam in underdense plasma

ARVINDER SINGH AND NAVEEN GUPTA
Department of Physics, National Institute of Technology, Jalandhar, India
(Received 18 April 2015; Accepted 24 June 2015)

Abstract

This paper presents theoretical investigation of effect of relativistic self-focusing of cosh-Gaussian (ChG) laser beam on second-harmonic generation in an underdense plasma. Steep transverse density gradients are produced in the plasma by the electron plasma wave excited by relativistic self-focusing of ChG laser beam. The generated plasma wave interacts with the pump beam to produce its second harmonics. Following Jeffrey Wentzel Kramers Brillouin (J.W.K.B) approximation and moment theory the differential equation governing the evolution of spot size of laser beam with distance of propagation has been derived. The differential equation so obtained has been solved numerically by the Runge–Kutta method to investigate the effect of decentered parameter, intensity of laser beam as well as density of plasma on self-focusing of the ChG laser beam, and generation of its second harmonics. It has been observed that the peak intensity of the laser beam shifts in the transverse direction by changing the decentered parameter and a noticeable change is observed on focusing of the laser beam as well as on conversion efficiency of second harmonics.

Keywords: Cosh-Gaussian; Self-focusing; Underdense plasmas

1. INTRODUCTION

With the advent of high-power lasers, theoretical as well as experimental investigations of nonlinear interaction of intense laser beams with plasmas are gaining much interest among researchers due to its widespread importance in a number of novel applications, including laser-driven particle accelerators (Tajima & Dawson, 1979; Faure *et al.*, 2004; Geddes *et al.*, 2004; Mangles *et al.*, 2004), inertial confinement fusion (Deutsch *et al.*, 1996; Hora, 2007), X-ray lasers (Amendt *et al.*, 1991), harmonic generation (Sturrock *et al.*, 1965; Bulanov *et al.*, 1994; Lichters *et al.*, 1996; Willes *et al.*, 1996; Dromey *et al.*, 2009), etc. Propagation of laser beams through plasmas up to several Rayleigh lengths is an important prerequisite for successful realization of all these applications. During the propagation of intense laser beams through plasmas many nonlinear effects such as filamentation of laser beam, self-phase modulation, group velocity dispersion, relativistic self-focusing, etc. come into the picture. It is therefore essential to investigate some of these effects for the in-depth understanding of laser–plasma interaction physics.

Address correspondence and reprint requests to: Arvinder Singh, Department of Physics, National Institute of Technology, Jalandhar, India. E-mail: arvinder6@lycos.com

The inertial confinement fusion programs led to construction of lasers capable of reaching intensities over the range 10^{18}–10^{20} W/cm^2. When such a highly intense laser beam propagates through the plasma, the quiver velocity of plasma electrons becomes comparable to that of light in the vacuum, causing significant increase in their mass. Owing to the spatial intensity distribution of the laser beam along its wavefront, electrons will experience mass change according to their radial position. The mass change will translate into modification of dielectric properties of plasma due to which the plasma behave like a convex lens leading to self-focusing of the laser beam.

Harmonic generation of electromagnetic radiations in the laser-produced plasmas has become an important field of research due to its number of applications. The process of higher harmonic generation has strong influence on the nature of propagation of laser beams through plasmas. It allows the penetration of laser power to overdense regions and hence is a promising diagnostic tool for obtaining information of plasma parameters such as local electron density, electrical conductivity, opacity, expansion velocity, as reviewed by Teubner and Gibbon (2009). Harmonic generation can also be used to detect the presence of large electrical and magnetic fields, plasma waves, and the electron transport inside the target with the help of

interferometry or absorption spectroscopy. The second-harmonic generation is used to track the passage of high-intensity laser pulses through underdense plasma targets and also provides information about linear mode conversion of the laser beam into plasma wave near the critical layer (Stamper *et al.*, 1985). Owing to their high penetrating power, harmonic radiations also find applications in material and biological imaging.

Being already in an ionized state, the plasma is capable of handling very high electric fields and hence, offers a promising medium for producing higher harmonic radiations. There are a number of mechanisms through which one can generate higher harmonics of laser beams in plasmas. These mechanisms include resonance absorption (Erokhin *et al.*, 1969), parametric instabilities (Bobin, 1985), transverse density gradients associated with light filaments (Stamper *et al.*, 1985), ionization fronts (Brunel, 1990), and photon acceleration (Wilks *et al.*, 1989), through plasma wave excitation (Sodha *et al.*, 1978; Parashar & Pandey, 1992; Singh & Walia, 2011*a*, *b*). In the case of second-harmonic generation, the main mechanism is excitation of the electron plasma wave at pump frequency that interacts with the pump beam to produce its second harmonics.

Harmonic generation in the laser–plasma interaction has been investigated extensively both experimentally as well as theoretically by a number of workers (Kant *et al.*, 2004*a*, *b*, 2011, 2012; Singh & Gupta, 2015; Verma *et al.*, 2015). Burnett *et al.* (1977) observed harmonics up to 11th from planar solid targets. Carman *et al.* (1981*a*) observed harmonic orders up to 27, and then 49 in a second experiment (Carman *et al.*, 1981*b*). Hora and Ghatak (1985) derived and evaluated the second-harmonic resonance for perpendicular incidence at four times the critical density. Kant *et al.* (2004*a*, *b*) investigated the second-harmonic generation of short laser pulse in the plasma by taking into consideration the effect of pulse slippage. Kaur *et al.* (2009) investigated the resonant second-harmonic generation of Gaussian laser beam in collisional magnetoplasma. Agarwal *et al.* (2001) studied the resonant second-harmonic generation of a millimeter wave in plasma in the presence of magnetic wiggler. The wiggler provides an additional momentum for the generation of harmonic photon. Singh et al. investigated the effect of self-focusing of the Gaussian laser beam on second-harmonic generation in collisional (Singh & Walia, 2011*a*), collisionless (Singh & Walia, 2011*b*), and relativistic (Singh & Walia, 2013) plasmas using the moment theory approach (Lam *et al.*, 1975, 1977). Jha & Aggarwal (2014) investigated the second-harmonic generation of p-polarized laser beam in underdense plasma.

Laser beams with different intensity profiles behave differently in plasmas (Nanda *et al.*, 2013). Literature review reveals the fact that most of the theoretical investigations on second-harmonic generation have been carried out under the assumption of uniform laser beam or laser beams having Gaussian distribution of intensity along their wavefronts. In contrast to this picture, a new class of laser beams known as cosh-Gaussian (ChG) laser beams has become the center of attraction to researchers because these beams possess high-power and low divergence in comparison to Gaussian beams. Recently in some publications (Patil *et al.*, 2012; Nanda & Kant, 2014), self-focusing of ChG laser beams has been reported with the help of the paraxial theory. The paraxial theory being local in character overemphasizes the field close to the beam axis. In ChG laser beams, most of the energy is concentrated in the off-axial region of wavefront as compared to the axial region. Moreover, for decentered parameter $b > 1$ of the ChG laser beam, maximum intensity appears in the outer lobes of the wavefront as compared to the intensity on the axis of the laser beam (cf. Fig. 1). In view of this, it is not appropriate to the Taylor expand nonlinear part of the dielectric function about the axis of ChG laser beam. To overcome this major drawback the moment theory has been used for the analysis of propagation characteristics of ChG laser beam in which the entire nonlinear part of the dielectric function is taken into consideration. The aim of this paper is to investigate, for the first time, the effect of relativistic self-focusing of the ChG laser beam in plasma and its effect on the second-harmonic generation.

The systematic organization of this paper is as follows:

In Section 2, the differential equation describing the evolution of spot size of the laser beam with distance of propagation has been derived. In Section 3, the conditions for uniform wave-guide propagation of the laser beam have been obtained. Section 4 describes the generation of electron plasma wave (EPW) at pump frequency, and in Section 5 the equation for conversion efficiency of the second harmonics has been obtained. Lastly in Section 6, the detailed discussion of the results obtained has been presented.

2. EVOLUTION OF SPOT SIZE OF LASER BEAM

Consider the propagation of an intense, circularly polarized laser beam having an electric field vector

$$\mathbf{E}(r, z, t) = E_0(r, z)e^{\iota(\omega_0 t - k_0 z)}(\mathbf{e}_x + \iota\mathbf{e}_y) \tag{1}$$

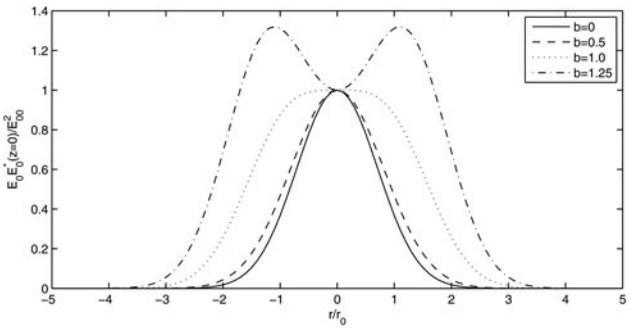

Fig. 1. Variation of the normalized intensity $\left(E_0.E_0^*|_{z=0}/E_{00}^2\right)$ with normalized radial distance r/r_0 for different values of b viz. $b = 0, 0.5, 1.0, 1.25$

https://doi.org/10.1017/S0263034615000749 Published online by Cambridge University Press

through an underdense plasma having the dielectric constant

$$\epsilon = 1 - \frac{\omega_p^2}{\omega_0^2}, \tag{2}$$

where $\mathbf{e}_x$ and $\mathbf{e}_y$ are the unit vectors along the x- and y-axes, respectively, $E_0(r,z)$ is the slowly varying complex amplitude of the electric field of the laser beam and

$$\omega_p^2 = \frac{4\pi e^2 n_0}{m} \tag{3}$$

is the plasma frequency in the presence of laser beam; n_0 is the electron density; e and m, respectively, are the charge and effective mass of the electron.

Owing to the circular polarization of the field of laser beam, the plasma electrons move along the circular orbits with frequency ω_0 and due to high field associated with the laser beam the quiver speed of the electrons becomes comparable to that of light in the vacuum. Hence, the effective mass m of the electrons in Eq. (3) gets replaced by $m_0\gamma$, where m_0 is the rest mass of the electrons and γ is the relativistic Lorentz factor. Following Akhiezer and Polovin (1956), at equilibrium

$$-eE_0 = mv\omega_0$$

from which we get

$$\gamma = (1 + \beta E_0 E_0^*)^{1/2}, \tag{4}$$

where

$$\beta = \frac{e^2}{m_0^2 c^2 \omega_0^2} \tag{5}$$

is the coefficient of the relativistic nonlinearity. Hence, the effective dielectric function of the plasma can be written as

$$\epsilon = 1 - \frac{\omega_{p0}^2}{\omega_0^2}(1 + \beta E_0 E_0^*)^{-1/2}, \tag{6}$$

where

$$\omega_{p0}^2 = \frac{4\pi e^2 n_0}{m_0} \tag{7}$$

is the plasma frequency in the absence of laser beam. Equation (6) can be written as

$$\epsilon = \epsilon_0 + \phi(E_0 E_0^*), \tag{8}$$

where

$$\epsilon_0 = 1 - \frac{\omega_{p0}^2}{\omega_0^2} \tag{9}$$

is the linear part of the dielectric function, and

$$\phi(E_0 E_0^*) = \frac{\omega_{p0}^2}{\omega_0^2}\left(1 - \frac{1}{\gamma}\right) \tag{10}$$

is the nonlinear dielectric response of the plasma to the field of incident laser beam.

The electric field vector $\mathbf{E}$ of the laser beam satisfy the electromagnetic wave equation

$$\nabla^2 \mathbf{E} - \nabla(\nabla.\mathbf{E}) + \frac{\omega_0^2}{c^2}\epsilon \mathbf{E} = 0. \tag{11}$$

Even, if $\mathbf{E}$ has the longitudinal components, the polarization term $\nabla(\nabla.\mathbf{E})$ of Eq. (11) can be neglected provided $c^2/\omega_0^2 \left|(1/\varepsilon)\nabla^2 \ln \epsilon\right| \ll 1$. This will be valid if $\nabla_\perp\left((1/\epsilon)\nabla_\perp \epsilon\right) \ll k_0^2$, that is, the transverse gradient of the dielectric function is smaller as compared with the laser wavelength which implies that either the transverse dielectric variation is weak or the plasma is significantly underdense. We need only to stress that Eq. (11) is the nonlinear wave equation, since ϵ depends on field amplitude E_0 via Eq. (6). Under this approximation, Eq. (11) can be written as

$$\iota \frac{dE_0}{dz} = \frac{1}{2k_0}\nabla_\perp^2 E_0 + \frac{k_0}{2\varepsilon_0}\phi(E_0 E_0^*)E_0. \tag{12}$$

In deriving Eq. (12), the term d^2E_0/dz^2 has been neglected under the assumption that the wave-amplitude scale length along the longitudinal direction is much larger as compared to the characteristic scale in the transverse direction. Equation (12) is the well-known nonlinear Schrödinger wave equation and possesses a number of conserved quantities due to its symmetry properties. Among them two most important are:

$$I_0 = \int_0^{2\pi}\int_0^{\infty} E_0 E_0^* r dr d\theta, \tag{13}$$

$$I_2 = \int_0^{2\pi}\int_0^{\infty} \frac{1}{2k_0^2}(|\nabla_\perp E_0|^2 - F) r dr d\theta, \tag{14}$$

where

$$F(E_0 E_0^*) = \frac{1}{2\epsilon_0}\int_0^{E_0 E_0^*} \phi(E_0 E_0^*) d(E_0 E_0^*). \tag{15}$$

The first invariant I_0, which is a consequence of Gauge invariance, is merely a statement of conservation of energy of the laser beam and second invariant I_2 relates the wavefront curvature of the laser beam to plasma nonlinearity.

Now, from the definition of the second-order spatial moment of intensity distribution of the laser beam along its wave front, the mean-square radius of the laser beam is given by

$$\langle R^2(z)\rangle = \frac{1}{I_0}\int_0^{2\pi}\int_0^{\infty} r^2 E_0 E_0^* r dr d\theta. \tag{16}$$

Following the procedure of Lam et al. (1975, 1977), we get the following quasi-optic equation governing the evolution of mean-square radius of the laser beam with the distance

https://doi.org/10.1017/S0263034615000749 Published online by Cambridge University Press

of propagation.

$$\frac{d^2\langle R^2\rangle}{dz^2} = \frac{4I_2}{I_0} - \frac{4}{I_0}\int_0^{2\pi}\int_0^{\infty} Q(E_0E_0^*) r dr d\theta, \tag{17}$$

where

$$Q(E_0E_0^*) = \left[\frac{E_0E_0^*\phi(E_0E_0^*)}{2\epsilon_0} - 2F(E_0E_0^*)\right].$$

The intensity distribution of ChG laser beam along its wave front, at the plane of incidence ($z = 0$) is given by (Lu *et al.*, 1999; Konar *et al.*, 2007; Patil *et al.*, 2012)

$$E_0E_0^* = E_{00}^2 e^{-r^2/r_0^2}\cosh^2\left(\frac{b}{r_0}r\right), \tag{18}$$

where r_0 is the spot size of the laser beam at $z = 0$, E_{00} is the axial amplitude of the electric field of the laser beam, b/r_0 is the parameter associated with the cosh function, also called Cosh factor. For $b = 0$, the intensity distribution attains the usual Gaussian distribution. Equation (18) can be written as

$$E_0E_0^* = \frac{E_{00}}{4}e^{b^2}\left[e^{-((r/r_0)+b)^2} + e^{-((r/r_0)-b)^2} + 2e^{-((r^2/r_0^2)+b^2)}\right],$$

which implies that the ChG beam can be produced simply in the laboratory by superposition of two decentered Gaussian beams with same spot size and in phase, whose centers are located at the positions $(b/2, 0)$ and $(-b/2, 0)$, respectively.

For $z > 0$, energy-conserving ansatz for the intensity distribution of ChG laser beam propagating along the z-axis is given by

$$E_0E_0^* = \frac{E_{00}^2}{f^2}e^{-r^2/r_0^2f^2}\cosh^2\left(\frac{b}{r_0f}r\right), \tag{19}$$

where r_0f is the instantaneous spot size of the laser beam. Hence, the function f is termed as the dimensionless beam width parameter which is measure of both axial intensity and spot size of the laser beam. Using Eqs (10), (15), (16), and (19) in Eq. (17) we get the following differential equation governing the evolution of spot size of ChG laser beam with dimensionless distance of propagation $\left(\xi = z/k_0r_0^2\right)$.

$$\frac{d^2f}{d\xi^2} + \frac{1}{f}\left(\frac{df}{d\xi}\right)^2 = \left(\frac{1+e^{-b^2}(1-b^2)}{2(1+b^2)}\right)\frac{1}{f^3} - \left(\frac{e^{-b^2}}{1+b^2}\right) \times \left(\frac{\beta E_{00}^2}{f^2}\right)\left(\frac{\omega_{p0}^2r_0^2}{c^2}\right)(T_1 - bT_2), \tag{20}$$

where

$$T_1 = \int_0^{\infty} x^3\left\{1 + \frac{\beta E_{00}^2}{f^2}e^{-x^2}\cosh^2(bx)\right\}^{-3/2} e^{-2x^2}\cosh^4(bx)dr,$$

$$T_2 = \int_0^{\infty} x^2e^{-2x^2}\left\{1 + \frac{\beta E_{00}^2}{f^2}e^{-x^2}\cosh^2(bx)\right\}^{-3/2}\cosh^3(bx)\sinh(bx)dr,$$

$$x = \frac{r}{r_0f}.$$

For an initially plane wavefront, Eq. (20) is subjected to the boundary conditions $f = 1$ and $df/d\xi = 0$ at $\xi = 0$.

3. UNIFORM WAVEGUIDE PROPAGATION

For an initially plane wavefront $f = 1$ and $df/d\xi = 0$ at $\xi = 0$, the condition $d^2f/d\xi^2 = 0$ leads to the propagation of the ChG beam in uniform waveguide mode. The condition under which this occurs is termed as critical condition. By substituting $df/d\xi = d^2f/d\xi^2 = 0$ into Eq. (20), we obtain the following relation between the dimensionless equilibrium beam width $r_e = \omega_{p0}r_0/c$ and critical beam intensity βE_{00}^2

$$r_e = \left(\frac{1 - b^2 + e^{b^2}}{4\beta E_{00}^2}\right)^{1/2}\frac{1}{\sqrt{T_1' - bT_2'}}, \tag{21}$$

where

$$r_e = \frac{\omega_{p0}r_0}{c},$$

$$T_1' = \int_0^{\infty} x^3\left\{1 + \beta E_{00}^2e^{-x^2}\cosh^2(bx)\right\}^{-3/2} e^{-2x^2}\cosh^4(bx)dr,$$

$$T_2\prime = \int_0^{\infty} x^2e^{-2x^2}\left\{1 + \beta E_{00}^2e^{-x^2}\cosh^2(bx)\right\}^{-3/2}\cosh^3(bx)\sinh(bx)dr.$$

Equation (21) can be depicted on the $(\beta E_{00}^2, r_e)$ plane and is generally referred to as the critical power curve or, simply the critical curve. If the initial value of βE_{00}^2 and r_e of the laser beam are such that the point $(\beta E_{00}^2, r_e)$ lies on the critical curve, then the value of $d^2f/d\xi^2$ will vanish at $\xi = 0$. Since the initial value of $df/d\xi$ (in the case of plane wavefront) is zero, the value of $df/d\xi$ continues to be zero as the beam propagates through the plasma. Hence, the value of f, which is unity $(=1)$ at $\xi = 0$, will remain unchanged. The beam thus propagates without any change in its width. This regime is known as uniform waveguide propagation.

If the point $(\beta E_{00}^2, r_e)$, corresponding to initial normalized beam intensity and beam radius, lies below the critical curve, then $d^2f/d\xi^2 > 0$ and hence the spot size of the laser beam increases as it propagates through the plasma; whereas if the point $(\beta E_{00}^2, r_e)$ lie above the critical curve, then $d^2f/d\xi^2 < 0$ and hence the spot size of the laser beam decreases with the distance of propagation.

https://doi.org/10.1017/S0263034615000749 Published online by Cambridge University Press

4. PLASMA WAVE GENERATION

In the dynamics of excitation of EPW, it must be mentioned here that the contribution of ions is negligible because they only provide a static positive background, that is, only plasma electrons are responsible for the excitation of EPW. The background plasma density is modified via relativistic electron mass variation. Therefore, the amplitude of the EPW that depends on the background electron density gets strongly coupled to the laser beam.

The generated EPW is governed by the equation of continuity, equation of motion, equation of state, and Poisson's equation

$$\frac{\partial n}{\partial t} + \nabla(nv) = 0, \tag{22}$$

$$\frac{\partial(nv)}{\partial t} + \nabla(nv^2) + \frac{1}{m}\nabla P_e + \frac{neE}{m} = 0, \tag{23}$$

$$\frac{P_e}{n^3} = \text{constant}, \tag{24}$$

$$\nabla E = 4\pi(ZN_{0i} - n)e, \tag{25}$$

where n is the total electron density, that is, sum of the equilibrium plasma density and density perturbation associated with EPW, $\mathbf{E}$ is the sum of electric field vectors of the laser beam and self-consistent field associated with plasma wave, v is the velocity of electron fluid, P_e is the hydrodynamic pressure of the electron fluid, Z is the charge state of ions. Using the linear perturbation theory it can be shown that the plasma wave is governed by

$$-\omega_0^2 n' + v_{th}^2 \nabla^2 n' + \omega_p^2 n' = \frac{e}{m} n_0 \nabla E_0, \tag{26}$$

where $v_{th}^2 = 2K_0T_0/m_0$ is the thermal velocity of electrons and n' is the density perturbation associated with the plasma wave.

Taking

$$n' = n_1 e^{i(k_0 z - \omega_0 t)},$$

we get the following source term for the second-harmonic generation

$$n_1 = \frac{en_0}{m}\frac{E_{00}}{f}\frac{e^{-r^2/2r_0^2f^2}}{(\omega_0^2 - k_0^2 v_{th}^2 - \omega_p^2)} \times \left\{\frac{r}{r_0^2 f^2} - \frac{b}{r_0 f}\tanh\left(\frac{b}{r_0 f}r\right)\right\}\cosh^2\left(\frac{b}{r_0 f}r\right), \tag{27}$$

where $n_1(r, z)$ is the amplitude of the plasma wave.

5. SECOND-HARMONIC GENERATION

The wave equation governing the electric field E_2 of the second harmonic is given by (Singh *et al.*, 2011*a*, *b*, 2013)

$$\nabla^2 \mathbf{E}_2 + \frac{\omega_2^2}{c^2}\epsilon_2(\omega_2)\mathbf{E}_2 = \frac{\omega_{p0}^2}{c^2}\frac{n_1}{n_0}\mathbf{E}_0, \tag{28}$$

where $\omega_2 = 2\omega_0$ is the frequency of the second harmonic and ϵ_2 is the effective dielectric constant at second-harmonic frequency. From the above equation we get the expression for field E_2 of second harmonic as

$$E_2 = \frac{\omega_{p0}^2}{c^2}\frac{n_1}{n_0}\frac{E_0}{(k_2^2 - 4k_0^2)}. \tag{29}$$

Now the second-harmonic power can be written as

$$P_2 = \int_0^{2\pi}\int_0^{\infty} E_2 E_2^* r dr d\theta \tag{30}$$

also the power of the initial pump beam is given by

$$P_0 = \int_0^{2\pi}\int_0^{\infty} E_0 E_0^* r dr d\theta. \tag{31}$$

Defining the second-harmonic yield as

$$Y_2 = \frac{P_2}{P_0},$$

$$Y_2 = \frac{2}{9}\left(\frac{\omega_0^2 r_0^2}{c^2}\right)\left(\frac{\beta E_{00}^2}{f^4}\right)e^{-b^2}H, \tag{32}$$

where

$$H = \int_0^{\infty} e^{-2x^2}\frac{(x - b\tanh(bx))^2\cosh^4(bx)}{\left\{\frac{\omega_0^2 r_0^2}{c^2} - \epsilon_0\frac{v_{th}^2}{c^2}\frac{\omega_0^2 r_0^2}{c^2} - \frac{\omega_{p0}^2 r_0^2}{c^2} \times\left(1 + \frac{\beta E_{00}^2}{f^2}e^{-x^2}\cosh^2(bx)\right)^{-1/2}\right\}^2} dx. \tag{33}$$

6. DISCUSSION

Equations (20) and (32) respectively describe the variation of dimensionless beam width parameter f and the conversion efficiency $\eta_2\%$ of second harmonics of an intense ChG laser beam with dimensionless distance of propagation ξ, in an underdense plasma. These equations have been solved numerically for the following critical set of laser–plasma parameters:

$\omega_0 = 1.78 \times 10^{15}$ rad/s, $\lambda = 1.06$ μm, $r_0 =$ μm, and equilibrium plasma temperature $T_0 = 10^6$ K to analyze the effect of decentered parameter, intensity of laser beam as well as plasma density on relativistic self-focusing, and further its effect on conversion efficiency $\eta_2\%$ of second harmonics.

It is further mentioned that the right-hand side of Eq. (20) contains several terms, each representing some physical

https://doi.org/10.1017/S0263034615000749 Published online by Cambridge University Press

mechanism responsible for the evolution of beam during its propagation through plasma. First term on the right-hand side has its origin in the Laplacian ($\nabla_\perp^2$) in the nonlinear Schrödinger wave Eq. (12) and is responsible for diffraction divergence of the laser beam as it propagates through the medium, whereas the second term that arises under the effect of relativistic nonlinearity, is responsible for the convergence of the beam due to nonlinear refraction. This nonlinear term opposes the phenomenon of diffraction and depending on its numerical value as compared with the diffractive term, one can observe focusing/defocusing of the laser beam. It is the relative competition of various terms that ultimately determines the fate of spot size of the laser beam.

Figure 1 illustrates the normalized intensity profile ($E_0.E_0^*|_{z=0}/E_{00}^2$) versus r/r_0 of ChG laser beam for different values of decentered parameter b. For $b = 0$, the intensity profile of the ChG beam is similar to the Gaussian distribution and with increasing b (=0.5, 1.0) the profile becomes flat-topped. Moreover, with further increase in b (=1.25) a central dip appears in the intensity profile. Hence, it is observed from Figure 1 that with a suitable choice of decentered parameter b the intensity profile of ChG beam resembles to that of Gaussian, flat-topped, and dark hollow Gaussian laser beams.

Figure 2 illustrates normalized intensity of the ChG laser beam with normalized distance of propagation ξ and normalized radial distance r/r_0 for different values of decentered parameter $b = 0$, 0.50, 1.0, 1.50, respectively, in the absence of nonlinear refraction. The plots in Figure 2 depict that with an increase in the value of decentered parameter b the vacuum diffraction of the ChG laser beam decreases. This is solely due to the fact that for a given spot size r_0, the ChG laser beam with larger value of b possesses larger root mean square (*r.m.s*) beam width and hence diffract less, which supports the results of Konar et al. (2007).

Figures 3 and 4 show normalized intensity of the ChG laser beam in the plasma with normalized distance of propagation ξ and normalized radial distance r/r_0. It is observed that as the laser beam propagates through the plasma it gets filamented due to laser–plasma coupling through relativistic nonlinearity of electron mass. Figure 3 shows the generated filaments of the laser beam by taking fixed values of plasma density $\omega_{p0}^2 r_0^2/c^2 = 12.0$, laser intensity $\beta E_{00}^2 = 3.0$, and varying decentered parameter $b = 0$, 0.25, 0.50, 0.75. The plots in Figure 3(a)–(d) depict that an increase in the value of decentered parameter b from 0 toward 1 leads to enhanced localization of the filaments, that is, the generated filaments become more and more intense with an increase in the value of decentered parameter. This is due to the fact that for $0 < b < 1$ the intensity profile of the ChG laser beam resembles to that of flat-topped beam (cf. Fig. 1) as a result of which nonlinear refraction of most of the transverse part of the wavefront of the laser beam opposes the diffraction divergence. Hence, an increase in the value of b from 0 to 1 leads to localization of laser filaments. Hence, it is concluded from the present analysis that as we increase the value of decentered parameter for $0 \le b < 1$ the refractive term in Eq. (20) dominates the diffractive term and the refractive term is more pronounced in the case of flat-topped laser beams as compared to that of Gaussian beams. Figure 4 shows the generated filaments of the laser beam by taking fixed values of plasma density $\omega_{p0}^2 r_0^2/c^2 = 12.0$, laser intensity $\beta E_{00}^2 = 3.0$, and varying decentered parameter $b = 1.0$, 1.25, 1.50, 1.75. The plots in Figures 4(a)–(d) depict that for $b > 1$, with an increase

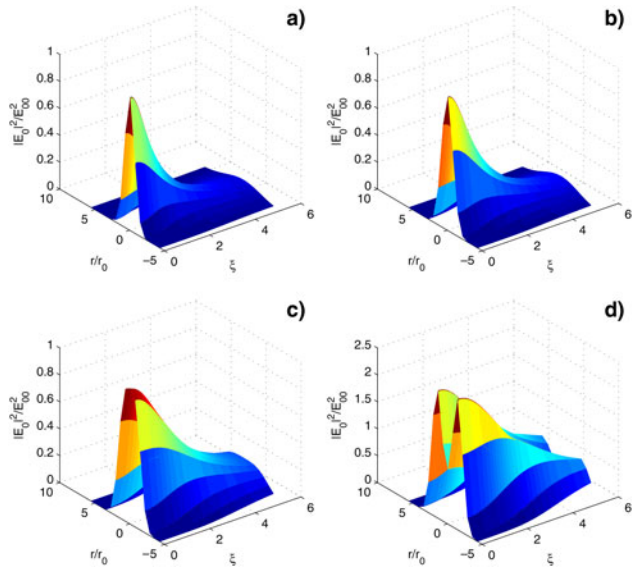

Fig. 2. Variation of the normalized laser beam intensity with normalized distance of propagation ξ and radial distance r/r_0, in the absence of nonlinear refraction, at different values of decentered parameter, (a) $b = 0$, (b) $b = 0.50$, (c) $b = 1.0$, and (d) $b = 1.50$, respectively.

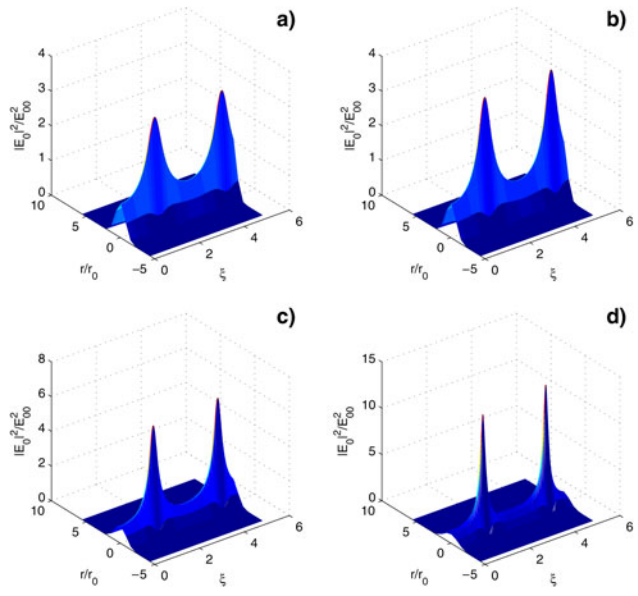

Fig. 3. Variation of the normalized laser beam intensity with normalized distance of propagation ξ and radial distance r/r_0, keeping $(\omega_{p0}r_0/c)^2 = 12$, $\beta E_{00}^2 = 3$ fixed and at different values of decentered parameter, (a) $b = 0$, (b) $b = 0.25$, (c) $b = 0.50$, (d) $b = 0.75$, respectively.

https://doi.org/10.1017/S0263034615000749 Published online by Cambridge University Press

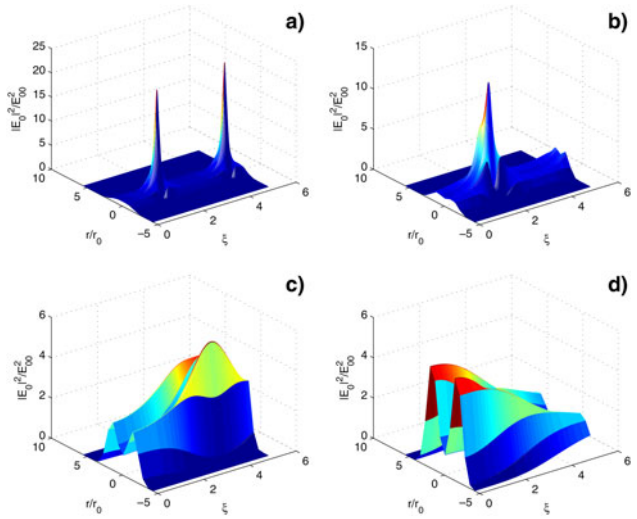

Fig. 4. Variation of the normalized laser beam intensity with normalized distance of propagation ξ and radial distance r/r_0, keeping $(\omega_{p0}r_0/c)^2 = 12$, $\beta E_{00}^2 = 3$ fixed and at different values of decentered parameter, (a) $b = 1.0$, (b) $b = 1.25$, (c) $b = 1.50$, and (d) $b = 1.75$, respectively.

in the value of b localization of the filaments decreases. It is observed from Figure 4 that as the value of decentered parameter b increases from 1 onwards up to 1.50, the diffractive term relatively dominates the refractive term but still maintaining the focusing character of the laser beam. As the value of b becomes more than 1.50 (or $b > 1.50$) the diffractive term completely dominates over the refractive term leading to complete defocusing of the laser beam.

Figure 5 shows the normalized intensity of the ChG laser beam in the plasma with normalized distance of propagation ξ and normalized radial distance r/r_0 for fixed values of decentered parameter $b = 0.25$, plasma density $\omega_{p0}^2 r_0^2/c^2 = 12$, and at varying values of laser intensity $\beta E_{00}^2 = 3.0, 3.50, 4.0, 4.50$. It is observed from Figure 5 that an increase in the laser intensity leads to enhanced intensity of the laser filaments. This is due to the fact that with an increase in the laser intensity the relativistic nonlinearity of electron mass also increases which leads to enhanced focusing of the laser beam.

Figure 6 shows the normalized intensity of the ChG laser beam in the plasma with normalized distance of propagation ξ and normalized radial distance r/r_0 for fixed values of decentered parameter $b = 0.25$, laser intensity $\beta E_{00}^2 = 3.0$, and at varying values of plasma density $\omega_{p0}^2 r_0^2/c^2 = 12, 13, 14, 15$. It is observed from Figure 6 that an increase in the plasma density leads to increase in the intensity of laser filaments. This is due to the fact that with an increase in plasma density the number of electrons contributing to self-focusing of the laser beam also increases.

Figure 7 describes the variation of equilibrium beam width r_e against the normalized intensity βE_{00}^2 for different values of decentered parameter b viz. $b = 0$, 0.50, 0.75, 1.0. It is observed from Figure 7 that for uniform waveguide propagation of ChG laser beam corresponding to the fixed value of equilibrium beam radius r_e, low-power lasers are required as we increase the value of decentered parameter for $0 \le b < 1$. So it is obvious from Figure 7 that highest laser power is required for the Gaussian laser beam to propagate in the uniform waveguide mode. Therefore, it is concluded that the flat-topped laser beams are more suitable for propagation in uniform waveguide mode at lowest laser power.

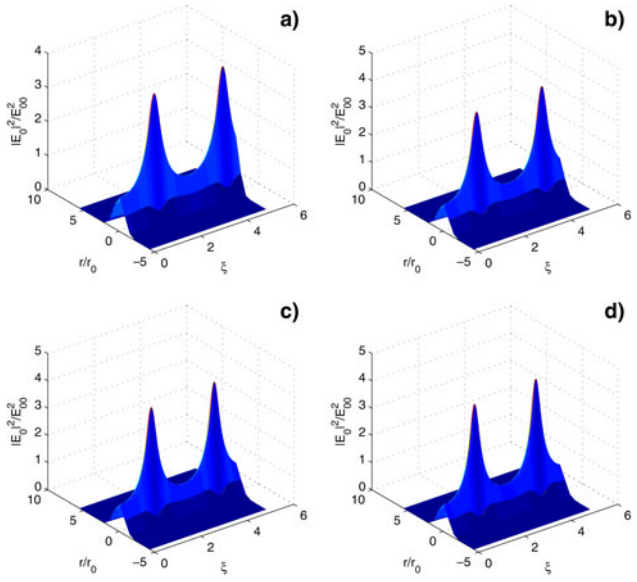

Fig. 5. Variation of the normalized laser beam intensity with normalized distance of propagation ξ and radial distance r/r_0, keeping $(\omega_{p0}r_0/c)^2 = 12$, $b = 0.25$ fixed and at different laser beam intensities, (a) $\beta E_{00}^2 = 3.0$, (b) $\beta E_{00}^2 = 3.50$, (c) $\beta E_{00}^2 = 4.0$, and (d) $\beta E_{00}^2 = 4.50$, respectively.

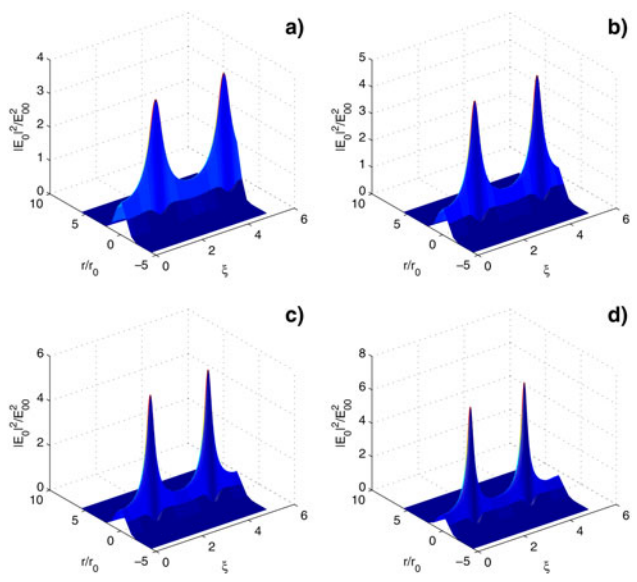

Fig. 6. Variation of the normalized laser beam intensity with normalized distance of propagation ξ and radial distance r/r_0, keeping $\beta E_{00}^2 = 3.0$, $b = 0.25$ fixed and at different plasma densities, (a) $(\omega_{p0}r_0/c)^2 = 12.0$, (b) $(\omega_{p0}r_0/c)^2 = 13.0$, (c) $(\omega_{p0}r_0/c)^2 = 14.0$, and (d) $(\omega_{p0}r_0/c)^2 = 15.0$, respectively.

https://doi.org/10.1017/S0263034615000749 Published online by Cambridge University Press

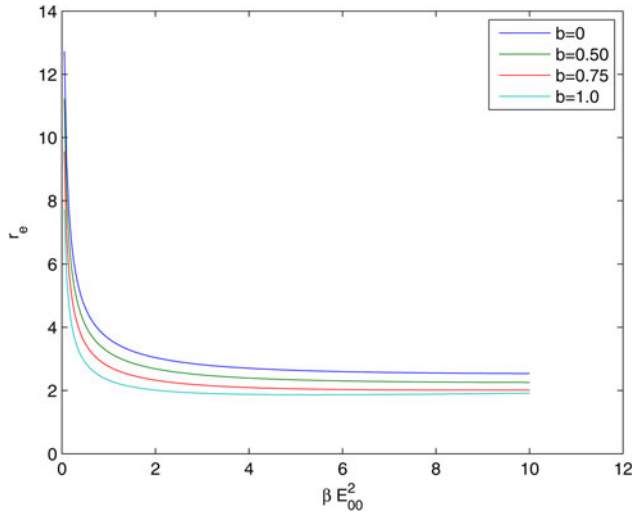

Fig. 7. Variation of the equilibrium beam width r_e against the normalized intensity βE_{00}^2 for different values of decentered parameter b viz. $b = 0$, 0.50, 0.75, 1.0.

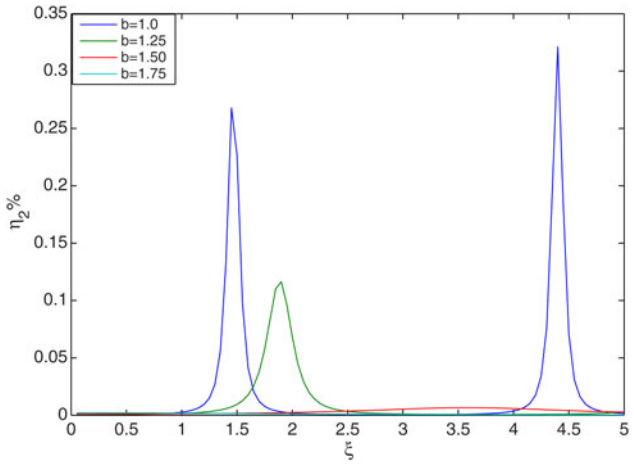

Fig. 9. Variation of the second-harmonic conversion efficiency η_2% against the normalized distance of propagation ξ for different values of decentered parameter b viz. $b = 1.0$, 1.25, 1.50, 1.75 at fixed laser intensity $\beta E_{00}^2 = 3.0$ and plasma density $(\omega_{p0} r_0/c)^2 = 12$.

Figures 8 and 9 describe the variation of the second-harmonic conversion efficiency η_2% against normalized distance of propagation ξ for fixed laser intensity $\beta E_{00}^2 = 3.0$, plasma density $\omega_{p0}^2 r_0^2/c^2 = 12.0$, and at varying values of the decentered parameter $b = 0$, 0.25, 0.50, 0.75 and 1.0, 1.25, 1.50, 1.75, respectively. It is seen that the conversion efficiency η_2% of the second harmonic oscillates as the laser beam propagates through the plasma and maximum conversion efficiency occurs at the focal regions. This is due to the fact that intensity gradients are very steep in the focal regions and hence, the plasma wave gets localized in these regions and consequently, the second-harmonic conversion efficiency is also more in these regions. The plots in Figures 8 and 9 depict that as the value of decentered parameter b increases from 0 to 1 there is substantial increase in the conversion efficiency η_2% of the second harmonics and with further increase of b from 1 onwards there is decrease in the conversion efficiency. This is due to the sensitiveness of conversion efficiency to the extent of localization of laser filaments. Greater is the localization of laser filaments, higher is the transverse density gradient in the focal region and hence higher is the harmonic yield and vice versa.

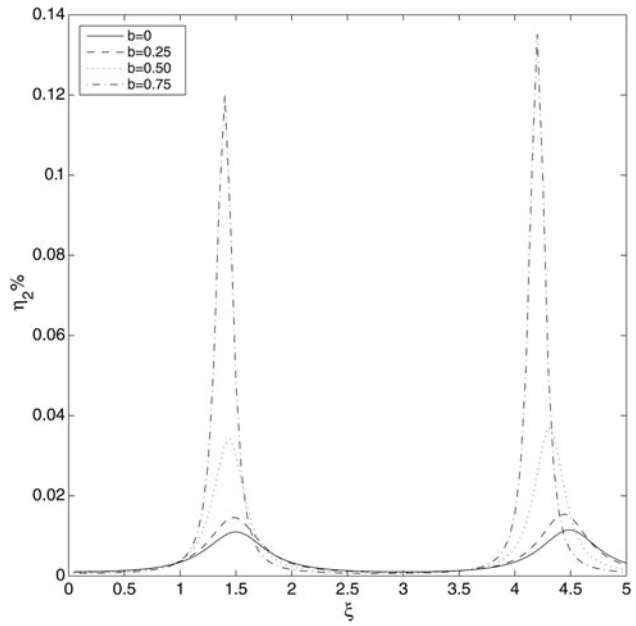

Fig. 8. Variation of the second-harmonic conversion efficiency η_2% against the normalized distance of propagation ξ for different values of decentered parameter b viz. $b = 0$, 0.25, 0.50, 0.75 at fixed laser intensity $\beta E_{00}^2 = 3.0$ and plasma density $(\omega_{p0} r_0/c)^2 = 12$.

Figure 10 describes the variation of the second-harmonic conversion efficiency η_2% against the normalized distance of propagation ξ for fixed values of decentered parameter $b = 0.25$, plasma density $\omega_{p0}^2 r_0^2/c^2 = 12.0$, and at varying values of laser intensity $\beta E_{00}^2 = 3.0$, 3.50, 4.0, 4.50. It is observed that with an increase in the intensity of the laser beam there is an increase in the conversion efficiency η_2%. This is due to the fact that the increase in the intensity of the incident laser beam enhances the intensity of laser filaments which further enhances the second-harmonic conversion efficiency η_2%.

Figure 11 describes the variation of the second-harmonic conversion efficiency η_2% against the normalized distance of propagation ξ for fixed values of decentered parameter $b = 0.25$, laser intensity $\beta E_{00}^2 = 3.0$, and at varying values of plasma density viz. $\omega_{p0}^2 r_0^2/c^2 = 12$, 13, 14, 15. It is observed that with an increase in the plasma density there is an increase in the second-harmonic conversion efficiency η_2%. This is due to the fact that an increase in plasma density leads to the enhanced intensity of laser filaments and therefore the transverse density gradient becomes very steep in the focal region, which leads to an increase in the amplitude of the plasma wave and hence the conversion efficiency η_2%.

https://doi.org/10.1017/S0263034615000749 Published online by Cambridge University Press

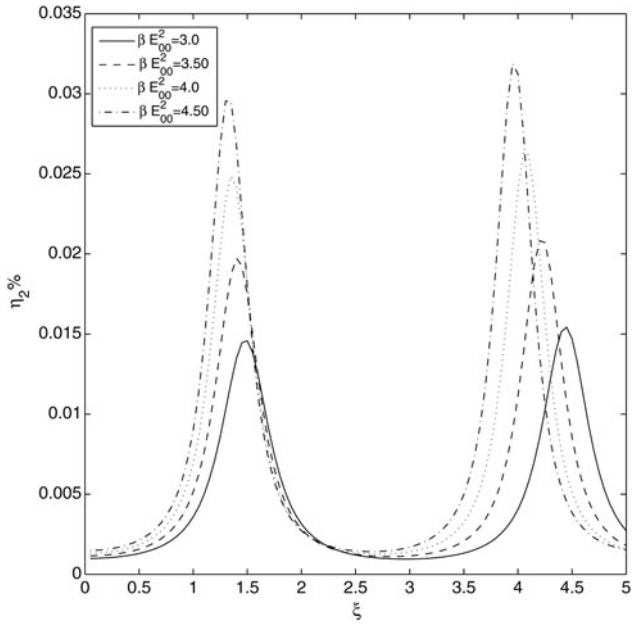

Fig. 10. Variation of the second-harmonic conversion efficiency $\eta_2\%$ against the normalized distance of propagation ξ for different laser intensities $\beta E_{00}^2 = 3.0, 3.50, 4.0, 4.50$ at fixed decentered parameter $b = 0.25$ and plasma density $(\omega_{p0} r_0/c)^2 = 12$.

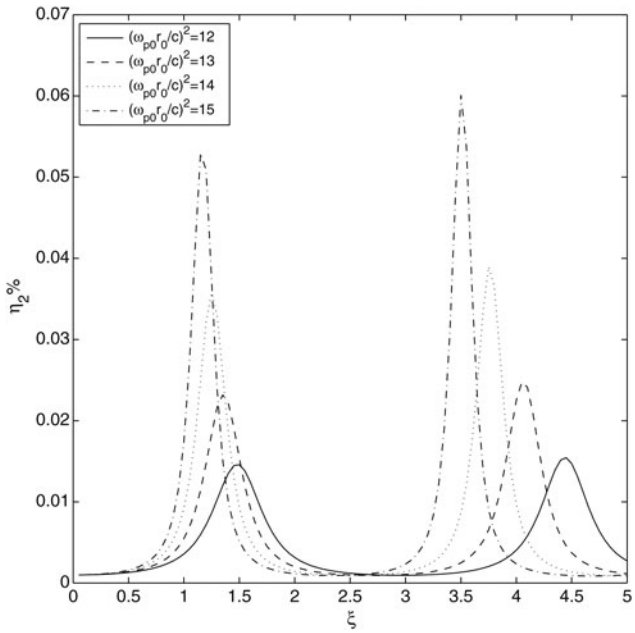

Fig. 11. Variation of the second-harmonic conversion efficiency $\eta_2\%$ against the normalized distance of propagation ξ for different plasma densities $(\omega_{p0} r_0/c)^2 = 12.0, 13.0, 14.0, 15.0$ at fixed decentered parameter $b = 0.25$ and laser intensity $\beta E_{00}^2 = 3.0$.

7. CONCLUSIONS

The present work delineates the effect of relativistic self-focusing of an intense ChG laser beam on the second-harmonic generation in underdense plasmas. Following important conclusions have been drawn from the present analysis:

- With an increase in decentered parameter for $0 \le b \le 1$, there is an increase in extent of self-focusing of the laser beam as well as of harmonic yield.
- With an increase in decentered parameter for $b > 1$, there is a decrease in extent of self-focusing of the laser beam as well as of harmonic yield.

These results are relevant to various contexts of laser–-plasma interaction physics. Besides its obvious relevance to the inertial confinement fusion, these results can also be helpful in other applications requiring laser beams with localized energy. The present results may serve as a guide for both experimental and theoretical investigations of laser–plasma interactions.

ACKNOWLEDGMENT

The authors are grateful to the Ministry of Human Resources and Development of India for providing financial assistance for carrying out this work.

REFERENCES

Agarwal, R.N., Pandey, B.K. & Sharma, A.K. (2001). Resonant second harmonic generation of a millimeter wave in a plasma filled waveguide. *Phys. Scr.* **63**, 243.

Akhiezer, A.I. & Polovin, R.V. (1956). Theory of wave motion of an electron plasma. *Sov. Phys.–JETP* **3**, 696–705.

Amendt, P., Eder, D.C. & Wilks, S.C. (1991). X-ray lasing by optical-field-induced ionization. *Phys. Rev. Lett.* **66**, 2589.

Bobin, J.L. (1985). High intensity laser plasma interaction. *Phys. Rep.* **122**, 173.

Brunel, F. (1990). Harmonic generation due to plasma effects in a gas undergoing multiphoton ionization in the high-intensity limit. *J. Opt. Soc. Am. B* **7**, 521.

Bulanov, S.V., Naumova, N.M. & Pegoraro, F. (1994). Interaction of an ultrashort, relativistically strong laser pulse with an overdense plasma. *Phys. Plasmas* **1**, 745.

Burnett, N.H., Baldis, H.A., Richardson, M.C. & Enright, G.D. (1977). Harmonic generation in CO_2 laser target interaction. *Appl. Phys. Lett.* **31**, 172–174.

Carman, R.L., Forslund, D.W. & Kindel, J.M. (1981*a*). Visible harmonic emission as a way of measuring profile steepening. *Phys. Rev. Lett.* **46**, 29.

Carman, R.L., Rhodes, C.K. & Benjamin, R.F. (1981*b*). Observation of harmonics in the visible and ultraviolet created in CO_2--laser-produced plasmas. *Phys. Rev. A* **24**, 2649.

Deutsch, C., Furukawa, H., Mima, K., Murakami, M. & Nishihara, K. (1996). Interaction physics of the fast ignitor concept. *Phys. Rev. Lett.* **77**, 2483–2486.

Dromey, B., Adams, D., Horlein, R., Nomura, Y., Rykovanov, S.G., Carroll, D.C., Foster, P.S., Kar, S., Markey, K., McKenna, P., Neely, D., Geissler, M., Tsakiris, G.D. & Zepf, M. (2009). Diffraction-limited performance and focusing of high harmonics from relativistic plasmas. *Nat. Phys.* **5**, 146.

Erokhin, N., Zakharov, V.E. & Moiseev, S.S. (1969). Second harmonic generation by an electromagnetic wave incident on inhomogeneous plasma. *Sov. Phys. – JETP* **29**, 101.

https://doi.org/10.1017/S0263034615000749 Published online by Cambridge University Press

Faure, J., Glinec, Y., Pukhov, A., Kiselev, S., Gordienko, S., Lefebvre, E., Rousseau, J.P., Burgy, F. & Malka, V. (2004). A laser–plasma accelerator producing monoenergetic electron beams. *Nature* **431**, 541–544.

Geddes, C.G.R., Toth, C., Tilborg, J.V., Esarey, E., Schroeder, C.B., Bruhwiler, D., Nieter, C., Cary, J. & Leemans, W.P. (2004). High-quality electron beams from a laser wakefield accelerator using plasma-channel guiding. *Nature* **431**, 538–541.

Hora, H. (2007). New aspects for fusion energy using inertial confinement. *Laser Part. Beams* **25**, 37–45.

Hora, H. & Ghatak, A.K. (1985). New electrostatic resonance driven by laser radiation at perpendicular incidence in superdense plasmas. *Phys. Rev. A* **31**, 3473.

Jha, P. & Aggarwal, E. (2014). Second harmonic generation by propagation of a p-polarized obliquely incident laser beam in underdense plasma. *Phys. Plasmas* **21**, 053107.

Kant, N., Gupta, D.N. & Suk, H. (2011). Generation of second-harmonic radiations of a self-focusing laser from a plasma with density-transition. *Phys. Lett. A* **375**, 3134–3137.

Kant, N., Gupta, D.N. & Suk, H. (2012). Resonant third-harmonic generation of a short-pulse laser from electron–hole plasmas. *Phys. Plasmas* **19**, 013101.

Kant, N. & Sharma, A.K. (2004*a*). Effect of pulse slippage on resonant second harmonic generation of a short pulse laser in a plasma. *J. Phys. D: Appl. Phys.* **37**, 998.

Kant, N. & Sharma, A.K. (2004*b*). Resonant second-harmonic generation of a short pulse laser in a plasma channel. *J. Phys. D: Appl. Phys.* **37**, 2395.

Kaur, S., Sharma, A.K. & Salih, H.A. (2009). Resonant second harmonic generation of a Gaussian electromagnetic beam in a collisional magnetoplasma. *Phys. Plasmas* **16**, 042509.

Konar, S., Mishra, M. & Jana, S. (2007). Nonlinear evolution of cosh-Gaussian laser beams and generation of flat top spatial solitons in cubic quintic nonlinear media. *Phys. Lett. A* **362**, 505–510.

Lam, J.F., Lippmann, B. & Tappert, F. (1975). Moment theory of self-trapped laser beams with nonlinear saturation. *Opt. Commun.* **15**, 419–421.

Lam, J.F., Lippmann, B. & Tappert, F. (1977). Self-trapped laser beams in plasma. *Phys. Fluids* **20**, 1176–1179.

Lichters, R., Vehn, J.M. & Pukhov, A. (1996). Short-pulse laser harmonics from oscillating plasma surfaces driven at relativistic intensity. *Phys. Plasmas* **3**, 3425.

Lu, B., Ma, H. & Zhang, B. (1999). Propagation properties of cosh-Gaussian beams. *Opt. Commun.* **164**, 165–170.

Mangles, S.P.D., Murphy, C.D., Najmudin, Z., Thomas, A.G.R., Collier, J.L., Dangor, A.E., Divall, E.J., Foster, P.S., Gallacher, J.G., Hooker, C.J., Jaroszynski, D.A., Langley, A.J., Mori, W.B., Norreys, P.A., Tsung, F.S., Viskup, R., Walton, B.R. & Krushelnick, K. (2004). Monoenergetic beams of relativistic electrons from intense laser–plasma interactions. *Nature* **431**, 535–538.

Nanda, V. & Kant, N. (2014). Strong self-focusing of a cosh-Gaussian laser beam in collisionless magneto-plasma under plasma density ramp Strong self-focusing of a cosh-Gaussian laser beam in collisionless magneto-plasma under plasma density ramp. *Phys. Plasmas* **21**, 072111–072117.

Nanda, V., Kant, N. & Wani, M.A. (2013). Sensitiveness of decentered parameter for relativistic self-focusing of hermite-cosh-Ggaussian laser beam in plasma. *IEEE Trans. Plasma Sci.* **41**, 2251–2256.

Parashar, J. & Pandey, H.D. (1992). Second-harmonic generation of laser radiation in a plasma with a density ripple. *IEEE Trans. Plasma Sci.* **20**, 996.

Patil, S.D., Takale, M.V., Navare, S.T., Fulari, V.J. & Dongare, M.B. (2012). Relativistic self-focusing of cosh-Gaussian laser beams in a plasma. *Opt. Laser Technol.* **44**, 314–317.

Singh, A. & Gupta, N. (2015). Second harmonic generation by relativistic self-focusing of q-Gaussian laser beam in preformed parabolic plasma channel. *Phys. Plasmas* **22**, 013102.

Singh, A. & Walia, K. (2011*a*). Self-focusing of Gaussian laser beam through collisional plasmas and its effect on second harmonic generation. *Laser Part. Beams* **29**, 407.

Singh, A. & Walia, K. (2011*b*). Self-focusing of Gaussian laser beam through collisionless plasmas and its effect on second harmonic generation. *J. Fusion Energ.* **30**, 555–560.

Singh, A. & Walia, K. (2013). Effect of self-focusing of Gaussian laser beam on second harmonic generation in relativistic plasma. *J. Fusion Energ.* **33**, 83–87.

Sodha, M.S., Sharma, J.K., Tewari, D.P., Sharma, R.P. & Kaushik, S.C. (1978). Plasma wave and second harmonic generation. *Plasma Phys.* **20**, 825.

Stamper, J.A., Lehmberg, R.H., Schmitt, A., Herbst, M.J., Young, F.C., Gardner, J.H. & Obenshain, S.P. (1985). Evidence in the second-harmonic emission for self-focusing of a laser pulse in a plasma. *Phys. Fluids* **28**, 2563–2569.

Sturrock, P.A., Ball, R.H. & Baldwin, D.E. (1965). Radiation at the plasma frequency and its harmonic from a turbulent plasma. *Phys. Fluids* **8**, 1509.

Tajima, T. & Dawson, J.M. (1979). Laser electron accelerator. *Phys. Rev. Lett.* **43**, 267–270.

Teubner, U. & Gibbon, P. (2009). High-order harmonics from laser-irradiated plasma surfaces. *Rev. Mod. Phys.* **81**, 445–479.

Verma, N.K., Agrawal, E. & Jha, P. (2015). Phase-matched second-harmonic generation via laser plasma interaction. *Euro Phys. Lett.* **109**, 15001.

Wilks, S.C., Dawson, J.M., Mori, W.B., Katsouleas, T. & Jones, M.E. (1989). Photon accelerator. *Phys. Rev. Lett.* **62**, 2600.

Willes, A.J., Robinson, P.A. & Melrose, D.B. (1996). Second harmonic electromagnetic emission via Langmuir wave coalescence. *Phys. Plasmas* **3**, 149.